

Local fluctuation effects in coupled small superconducting particles

R. C. Ward, S. Cremer,* and E. Šimánek

Department of Physics, University of California, Riverside, California 92521

(Received 21 October 1977)

A phenomenological Ginzburg-Landau treatment of a necklace of Josephson-coupled small particles is presented. The effective local gap Δ and the relaxation rate of the order parameter Γ are calculated within the Hartree approximation. These values are used to obtain the nuclear spin-lattice relaxation time T_1 . The model explains the different size dependence in the $T_1(T)$ measurements on Sn and Al small particles.

I. INTRODUCTION

In recent years there has been renewed interest in the electronic properties of small (zero-dimensional) superconducting particles. The fluctuation properties of a zero-dimensional superconductor of volume Ω are characterized by the parameter $\delta = (1/N_0\Omega)/k_B T_c$, which is the ratio of the mean electron-energy-level spacing to the characteristic energy $k_B T_c$. N_0 is the electronic density of states at the Fermi level and T_c is the bulk mean-field superconducting transition temperature.

One of the local electronic properties of great interest is the nuclear spin-lattice relaxation time T_1 . Early measurements of T_1 on small Al particles done by Masuda and Redfield¹ did not show a diverging relaxation rate $1/T_1$ as expected from the theoretical predictions of Maki *et al.*² Following the renormalization scheme of Patton,³ Šimánek *et al.*⁴ proposed a theory which was in agreement with the Masuda-Redfield data.¹ However, the agreement at low temperatures appeared to be fortuitous since it did not use a proper form for the effective gap $\Delta(T)$. Indeed, subsequent measurements of T_1 for smaller Al particles⁵ cannot be reconciled with the theory of Ref. 4 at lower temperatures.

Later measurements of $T_1(T)$ on Sn and Al particles by Kobayashi *et al.*⁶ which were done in relatively strong (for Al!) magnetic fields of 5–10 kOe (a) exhibited a much stronger size dependence for Al than for Sn particles, and (b) showed near T_c a more pronounced dip for Sn than for the same-size Al particles. Sone's microscopic theory,⁷ which includes the effect of the Zeeman energy splitting due to the magnetic field H , in spite of succeeding to explain the general features of the $T_1(T)$ data on Al, does not account for the dip near $T \simeq T_c$. This can be attributed to an overestimate of fluctuations in the smaller-sized particles. Recent measurements on Al particles in relatively low fields (0–1.2 kOe) again show a definite dip structure near T_c .⁸

In this paper we propose a model that includes

the effect of Josephson coupling between particles to account for the more pronounced dip structure of $T_1(T)$ near T_c , and to explain the differences between the results for Sn and Al particles [see (a) and (b) above]. It is expected that coupling should increase the effective volume, leading to a depression of the order-parameter fluctuations and, consequently, to the enhanced dip structure in $T_1(T)$ near T_c . Such couplings are expected since the particles form chains as a result of strong van der Waals forces between them. These chains or necklaces (closed chains) appear in electron micrographs of samples of small particles.⁸

An important feature which distinguishes Sn from Al particles is the presence of large spin-orbit coupling in Sn.⁹ We believe that the difference in $T_1(T)$ cannot be explained by the spin-orbit interaction. The latter tends to compete with the Zeeman splitting due to the external magnetic field, which is always present in the above reported experiments (see Ref. 6). Thus, it is expected that the $T_1(T)$ curves for Sn, in the presence of spin-orbit coupling, will show a stronger size dependence than was seen experimentally [see (a) above].

II. EFFECTIVE GAP

Following Deutscher *et al.*,¹⁰ we introduce the Ginzburg-Landau free-energy functional for N equal-volume (Ω) coupled particles arranged on a necklace,

$$\begin{aligned} \frac{F[\Psi]}{\Omega} = & N_0 \sum_{i=1}^N (A |\Psi_i|^2 + \frac{B}{2} |\Psi_i|^4) \\ & + N_0 \sum_{\substack{i,j \\ i < j}} C_{ij} |\Psi_i - \Psi_j|^2, \end{aligned} \quad (2.1)$$

where Ψ_i is the time-dependent superconducting complex order parameter for the i th particle. $A = T/T_c - 1$ and $B = [b_0 + (b_1 - b_0)T/T_c]/T_c^2$, with $b_0 = (1.76)^{-2}$ and $b_1 = 0.106$. The above form for $B(T)$ is chosen to simulate, in the bulk limit, the BCS result for $\Delta(T)$ at low temperatures. The last term in expression (2.1) represents the Josephson

coupling between nearest neighbors. Assuming a homogeneous coupling,¹⁰ $C_{ij} = C$, the relation between C and the size parameter δ is given by

$$C = (10^3/R_N)\delta \equiv \alpha\delta, \quad (2.2)$$

where R_N is the interparticle junction normal resistance (in ohms). Due to difficulties in correctly measuring the resistance R_N in powders of small particles, one has only an order of magnitude estimate of the parameter α defined by Eq. (2.2). Below we use $\alpha = 1$ to characterize the strongly coupled Sn particles. This value is consistent with resistivity measurements on compressed Sn powders.¹¹

To calculate the effective gap of one particle, $\Delta = (\langle |\Psi_i|^2 \rangle_N)^{1/2}$, we use the Hartree approximation of the free-energy functional (2.1),

$$F_H = \frac{1}{T_c\delta} \left(\sum_{i=1}^N (A + B\Delta^2 + 2C) |\Psi_i|^2 - C \sum_{\substack{i,j \\ i < j}}^N (\Psi_i^* \Psi_j + \Psi_j^* \Psi_i) \right). \quad (2.3)$$

For an isolated particle ($C = 0$) the thermodynamic averages can be calculated exactly.¹² However, the Hartree approximation for Δ is not significantly different from the exact result, and therefore, we use this approximation to linearize the free-energy functional for the case of coupled particles ($C \neq 0$).

Using the usual matrix formalism, $\langle |\Psi_i|^2 \rangle_N$ are given by

$$\langle |\Psi_i|^2 \rangle_N / T_c^2 = \delta(T/T_c) \det \tilde{Q}_{N-1} / \det \tilde{P}_N. \quad (2.4)$$

The nonzero elements of the symmetric matrix \tilde{P}_N are defined by

$$P_{ii} = D; \quad P_{i,i+1} = -C; \quad P_{1,N} = -C, \quad (2.5)$$

where $D = A + B\langle |\Psi_i|^2 \rangle + 2C$. The matrix \tilde{Q}_N is obtained from \tilde{P}_N simply by setting the "closing chain" elements $P_{1,N} = P_{N,1} = 0$. The determinants $\det \tilde{P}_N$ and $\det \tilde{Q}_N$ satisfy

$$\det \tilde{P}_N = \det \tilde{Q}_N - C^2 \det \tilde{Q}_{N-2} - 2C^N, \quad (2.6a)$$

$$\det \tilde{Q}_N = +D \det \tilde{Q}_{N-1} - C^2 \det \tilde{Q}_{N-2}, \quad (2.6b)$$

where $\det \tilde{Q}_1 = D$, and $\det \tilde{Q}_2 = D^2 - C^2$.

It can be shown that for N strongly coupled particles ($C \rightarrow \infty$) the effective gap is given by the equation

$$\Delta_\infty^2 (A + B\Delta_\infty^2) = TT_c (\delta/N), \quad (2.7)$$

where the equation for the effective gap of an isolated particle Δ_0 is obtained from Eq. (2.7) with $N = 1$. Taking the limit $N \rightarrow \infty$ in Eq. (2.7) we obtain $\Delta_\infty^2 = 0$ for $T \geq T_c$ and $\Delta_\infty^2 = -A/B$ for $T \leq T_c$ which is the BCS bulk limit. (The same result is obtained

for Δ_0 by taking the limit $\delta \rightarrow 0$.) Finally, at high temperatures ($T > T_c$) where $B\Delta_\infty^2 \ll A$, Δ_∞^2 is simply given by Δ_0^2/N , i.e., the effective volume of a strongly coupled particle increases N times.

III. THE ORDER-PARAMETER RELAXATION RATE

The equation of motion for the order parameter Ψ_i of the i th particle, is

$$\frac{d}{dt} \Psi_i^*(t) + \frac{8T}{\pi N_0} \frac{\partial F_H}{\partial \Psi_i} \frac{1}{\Omega} = h_i(t), \quad (3.1)$$

where the Gaussian-random forces h_i have (via the equipartition theorem) the correlation function

$$\langle h_i^*(t) h_j(0) \rangle = (2\gamma T / N_0 \Omega) \delta_{ij} \delta(t); \quad \gamma = 8T/\pi.$$

The power spectrum matrix¹³ of the correlation functions $G_{ij}^N(t) = \langle \Psi_i^*(t) \Psi_j(0) \rangle_N / T_c^2$ is obtained as

$$\tilde{G}(\omega) = 2\delta\gamma(T/T_c) [\tilde{P}_N(-i\omega) \tilde{P}_N(i\omega)]^{-1} \quad (3.2)$$

where the "admittance" matrix $\tilde{P}_N(i\omega)$ is obtained from \tilde{P}_N by replacing D by $(\gamma D + i\omega)$ and C by γC .

In the case of an isolated particle, the time dependence of the correlation function $\langle \Psi^*(t) \Psi(0) \rangle$ is exponential with the order-parameter relaxation rate Γ_0 given by $\Gamma_0 = \gamma(A + B\Delta_0^2)$.

When N particles are coupled, the system can be excited in N normal modes Γ_i ($i = 1, N$) given by the (purely imaginary) poles of the matrix element $G_{11}^N(\omega)$.¹⁴ It can be shown that the lowest normal mode Γ_1 , for every N , is given by the expression $\Gamma_1 = \gamma(A + B\Delta^2)$, similar to the expression for Γ_0 .

The effective order-parameter relaxation rate Γ is obtained, for a given N , by fitting the function $G_{11}^N(\omega)$ to a Lorentzian $\Gamma/(\omega^2 + \Gamma^2)$. At very low temperatures, where $A + B\Delta^2 \sim 0$, the system prefers to stay in the lowest mode Γ_1 . As the temperature approaches T_c , the relative separation of the levels $(\Gamma_i - \Gamma_1)/\Gamma_1 \sim C/(A + B\Delta^2)$ decreases drastically (especially for relatively large particles), and therefore Γ reaches a value near the center of the "band" of normal relaxation modes. Since at these temperatures ($T \sim T_c$) all Γ_i are of the same order of magnitude, the level mixing seems to have little effect on the exponential behavior of $G_{11}^N(t)$. Therefore, the fit of $G_{11}^N(t)$ to a single Lorentzian of effective width Γ is satisfactory.¹⁵

Figure 1 shows the temperature dependence of the effective gap Δ (linear scale) together with that of the order parameter relaxation rate Γ , for $N = 2, 4$, and 8 . For comparison we plot also the isolated-particle and the mean-field results. It can be seen that as N increases, the Δ and Γ curves approach the mean-field result; only in the limit $C \rightarrow \infty$ will they match exactly.

In what follows we confine our attention to the case $N = 8$. For this case, N is large enough to

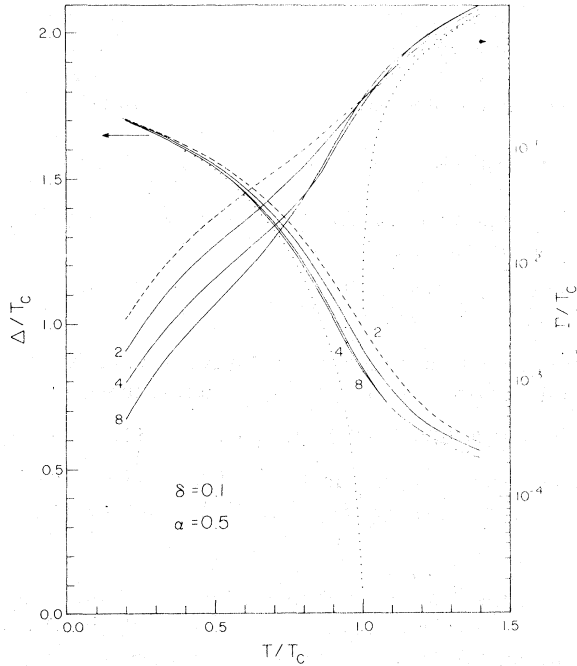


FIG. 1. Local effective gap Δ (linear scale) and the order-parameter relaxation rate Γ (logarithmic scale) as a function of the reduced temperature T/T_c for $\delta=0.1$ and $\alpha=0.5$ for $N=2, 4, 8$. The dashed (dotted) lines represent the single-particle (mean-field) results.

smooth out the effect of closing the chain but small enough to allow for a direct analytical calculation of the determinants and $G_{11}^N(\omega)$. Furthermore, in the following we will take $C=\delta$ ($\alpha=1.0$) to describe the strong coupling regime. At low temperatures at least, a coupling strength $C=\delta$ (i.e., $\alpha=1.0$) is strong enough to simulate the infinite coupling limit for the particular value $N=8$.

IV. NUCLEAR SPIN-LATTICE RELAXATION TIME

A. Pair-breaking effect of the magnetic field

The field pair breaking is accounted for in our scheme simply by replacing $A=T/T_c-1$ by

$$A \rightarrow A + \left(\frac{\pi \alpha_H}{8k_B T_c} \right) \frac{\Delta(T_c)}{\Delta(T)} = A + \eta_0 \frac{\Delta(T_c)}{\Delta(T)}, \quad (4.1)$$

where, following Maki,¹⁶ it is assumed that the pair-breaking mechanism is self-consistently controlled by the effective gap itself. The parameter α_H is defined as

$$\alpha_H = \frac{1}{15\pi} \left(\frac{e^2}{\hbar c} \right) \frac{v_F}{c} \left(\frac{1}{N_0 k_B T_c} \right) \frac{H^2}{\delta}, \quad (4.2)$$

where v_F is the Fermi velocity.¹⁷ In the general case, for any finite C , we calculate first $\Delta(T_c)$ and, using this value, $\Delta(H, T)$ and $\Gamma(H, T)$ are ob-

tained by solving Eqs. (2.4) and (2.5) with the replacement (4.1).¹⁸

The values of $\Delta(H=0, T)$ for $\delta=0.01, 0.1$, and 1.0 are exhibited in Fig. 2 together with the corresponding $\Delta(H, T)$ values calculated for Sn ($T_c=3.72^\circ\text{K}$) in an applied magnetic field of 5 kOe. As can be seen, the effect of the coupling is much stronger in the case of the smaller particles ($\delta=1.0$), whereas the effect of the magnetic field is almost unobservable. This is explained by the fact that the coupling drastically increases the effective volume of the smallest particles; while in the case of larger particles ($\delta=0.01$), the effective increase of the volume due to the coupling does not appreciably change their bulklike behavior. We note that the effect of the coupling is stronger for all δ values at temperatures around T_c . The effect of the field is simply explained by the δ dependence of α_H , which takes larger values as the bulk limit is approached.

The corresponding values for the effective relaxation rate Γ are presented in Fig. 3. The effect

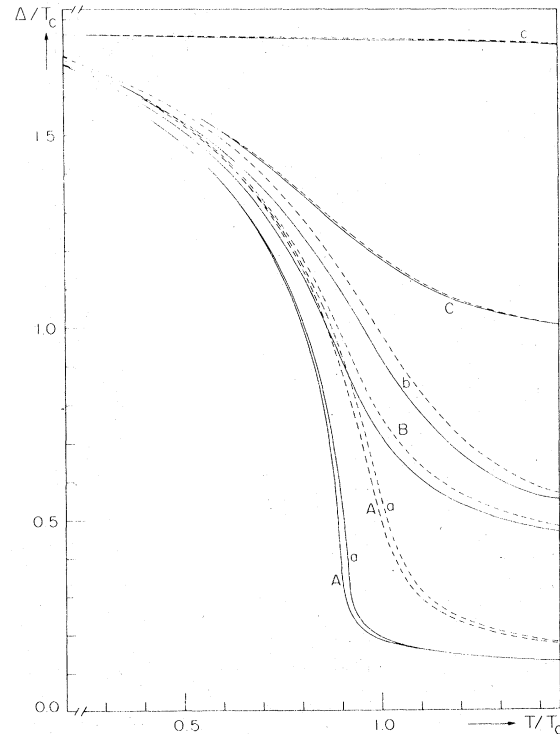


FIG. 2. Temperature dependence of the effective local gap $\Delta(T)$ for $H=0$ (dashed lines) and $H=5$ kOe (solid lines) calculated with $T_c=3.72^\circ\text{K}$ for Sn. The curves labeled by a ($\delta=0.01$), b ($\delta=0.1$), and c ($\delta=1.0$) represent the isolated particle case, whereas the respective curves A, B, C represent the case of eight coupled particles with $\alpha=1.0$.

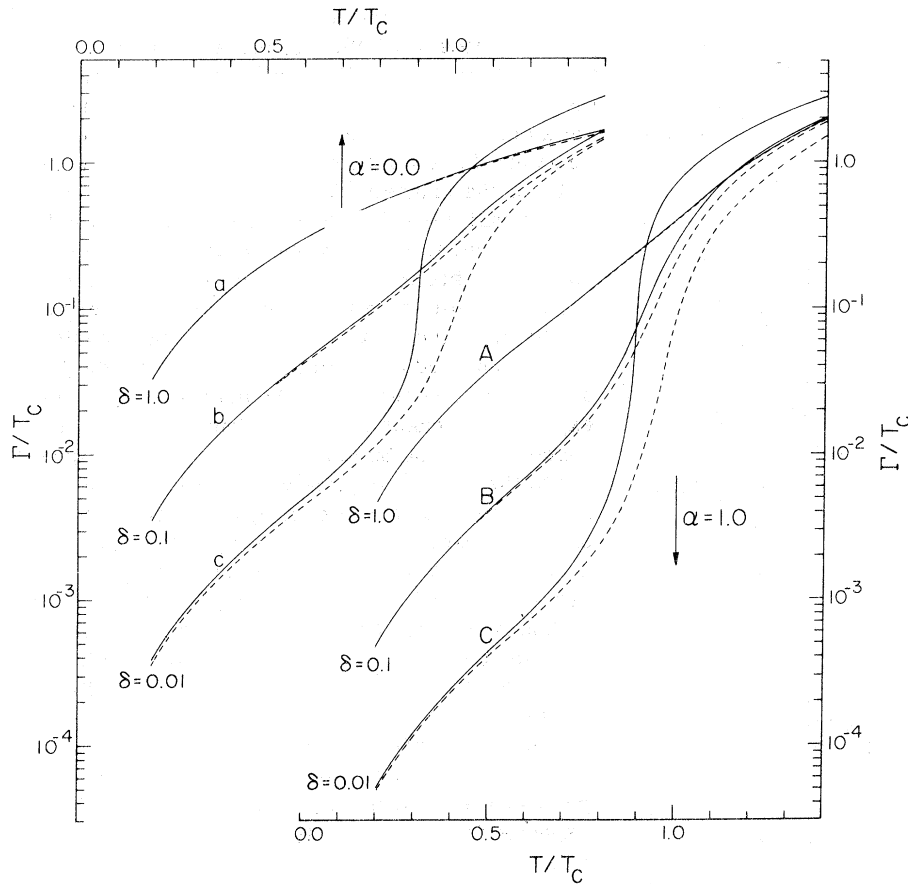


FIG. 3. Temperature dependence of the order-parameter relaxation rate Γ for the same cases presented in Fig. 4 for Δ . Note the shifted temperature scale for the cases $\alpha = 0.0$ and $\alpha = 1.0$.

of the coupling and of the magnetic field on the Γ values is similar to that for the effective gap. We point out that, in the case of an applied magnetic field, especially for larger particles ($\delta = 0.01$), the values for Γ become, at $T \geq T_c$, comparable to, or even larger than, the characteristic energy $k_B T_c$.

B. Nuclear spin-lattice relaxation rate

The phenomenological scheme developed above is applied here to obtain the nuclear spin-lattice relaxation time T_1 as a function of temperature, in the presence of coupling and magnetic field. The expression for T_1 is given by

$$\frac{T_{1n}(T_c)}{T_1} = \frac{T}{T_c} \int_{-\infty}^{\infty} dx \left(-\frac{\partial f_F}{\partial x} \right) \left[\text{Re} \left(\frac{z_p}{w_p} \right) \text{Re} \left(\frac{z_m}{w_m} \right) + \text{Re} \left(\frac{1}{w_p} \right) \text{Re} \left(\frac{1}{w_m} \right) \right], \quad (4.3)$$

where $z_{p,m} = [(Tx \pm \mu_B H) + i\Gamma/2]/\Delta$ and $w_{p,m} = (z_{p,m}^2 - 1)^{1/2}$. Expression (4.3) is a generalization of the result of Ref. 4 to include the Zeeman energy splitting due to the field H .¹⁹ This effect is important

since it strongly reduces the overlap of the spin-up and spin-down parts of the integrand in Eq. (4.3). We note that the field-induced pair breaking effect was taken into account previously in the effective-gap and relaxation-rate calculations.

We remark that in general the coupling between the particles can affect the spin-spin correlation function, and therefore via the spin susceptibility the $T_1(T)$ expression. However, since the normal spin susceptibility is mainly controlled by the Fermi wave number k_F , and the latter is much larger than the inverse Pippard coherence length $\xi(0)^{-1} \sim k_F(T_c/T_F)$, we expect that the effect of coupling on the $T_1(T)$ expression will be much smaller than on the Δ and Γ values.

The $T_1(T)$ results calculated for three different size particles ($\delta = 0.01, 0.1, 1.0$) are summarized in Fig. 4. Let us first discuss the effect of the field on the isolated particles case ($\alpha = 0.0$). As pointed out earlier, the magnetic field, via the pair-breaking effect, strongly decreases the value of Δ and increases the value of Γ for the larger ($\delta = 0.01$) size particles. Additionally, since at a given temperature the values of $\Delta(T)$ for the larger particles are smaller than for the smaller parti-

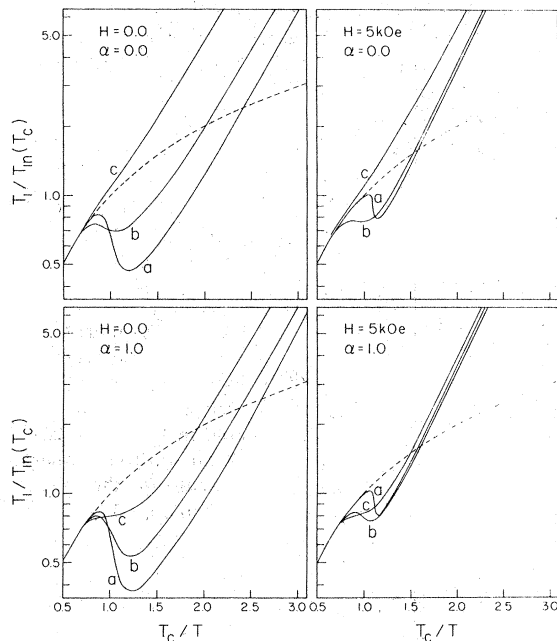


FIG. 4. Nuclear spin-lattice relaxation time T_1 as a function of T_c/T for (a) $\delta=0.01$, (b) $\delta=0.1$, and (c) $\delta=1.0$. The dashed curve in each plot represents the normal bulk behavior for $H=0.0$ and $\alpha=0.0$.

cles, the Zeeman energy splitting (proportional to $\mu_B H/\Delta$) is more effective in decreasing the value of the integral in Eq. (4.3). Therefore, the $T_1(T)$ curves for $\delta=0.01$ and $\delta=0.1$ are drastically shifted to higher values, whereas the $T_1(T)$ curve for the smallest particles is unchanged. Moreover, we can see that in this case ($H=5$ kOe, $\alpha=0.0$) the $\delta=0.01$, 0.1 curves become much closer together, especially in the low-temperature re-

gime. We turn now to the case of (strongly) coupled particles ($\alpha=1.0$). Again, it can be seen that the coupling between the particles mostly affects the $T_1(T)$ curve for the smallest particles, inducing a definite dip around $T \sim T_c$. Note that the dip structure for the larger particles is increased as well. If the magnetic field H is turned on, the larger particle $T_1(T)$ curves are shifted, as in the $\alpha=0.0$ case, to higher values such that all three curves are brought together. It should be pointed out that, while the differences near T_c are drastically diminished, they remain distinguishable.

The combined effect of the coupling and the field, as seen in the case $H=5$ kOe and $\alpha=1.0$, seems to explain the weaker size dependence of $T_1(T)$ measurements in the Sn particle case, which is pertinent to the strong coupling regime. In the case of Al, where α is orders of magnitude smaller than one, it is expected that the size dependence of the $T_1(T)$ curves will be more pronounced, as in the results for $H=5$ kOe and $\alpha=0.0$.²⁰

Finally, we remark that the present treatment is based on a somewhat idealized model which does not take into account the particle size distribution or fluctuations in the Josephson coupling strength between the particles. In addition, in real (packed) samples, the chains will cluster, producing a quasi-three-dimensional network.²¹ This effect is expected to enhance the tendency toward bulklike behavior.

ACKNOWLEDGMENTS

We acknowledge helpful discussions with Dr. D. E. MacLaughlin, Dr. J. A. Watrous, Dr. J. C. Hayward, and P.-K. Tse. This work was supported in part by ERDA Grant No. EY-76-S-03-0034 P.A. 233.

*Present address: Dept. of Physics, Nuclear Research Center-Negev, P. O. Box 9001, Beer-Sheva, Israel.

¹Y. Masuda and A. G. Redfield, Phys. Rev. **133**, A944 (1964).

²K. Maki, J. P. Hurault, and M. T. Béal-Monod, Phys. Lett. A **31**, 526 (1970). See also, J. P. Hurault, K. Maki, and M. T. Béal-Monod, Phys. Rev. B **3**, 762 (1971).

³B. R. Patton, Phys. Rev. Lett. **27**, 1273 (1971). See also, B. R. Patton, thesis (Cornell University, 1971) (unpublished).

⁴E. Šimánek, D. Imbro, and D. E. MacLaughlin, J. Low Temp. Phys. **11**, 787 (1973).

⁵S. Kobayashi, T. Takahashi, and W. Sasaki, J. Phys. Soc. Jpn. **31**, 1442 (1971).

⁶S. Kobayashi, T. Takahashi, and W. Sasaki, J. Phys. Soc. Jpn. **36**, 714 (1974).

⁷J. Sone, J. Low Temp. Phys. **23**, 699 (1976).

⁸D. E. MacLaughlin and P. K. Tse (unpublished).

⁹H. Shiba, J. Low Temp. Phys. **22**, 105 (1976).

¹⁰G. Deutscher, Y. Imry, and L. Gunther, Phys. Rev. B **10**, 4598 (1974). For a Gaussian treatment of the critical region for a system of coupled grains see G. Deutscher and Y. Imry, Phys. Lett. A **42**, 413 (1973). A pseudospin model of coupling between particles uniformly embedded in an oxide medium was developed much earlier by R. H. Parmenter [Phys. Rev. **154**, 353 (1967)].

¹¹Recent conductivity measurements on samples prepared by pressing Al and Sn small-particle powders prepared under the same oxidation conditions show normal resistivities which are of the order of $1 \Omega \text{ cm}$ for Sn and $10^8 \Omega \text{ cm}$ for Al [R. Gaupsas (private communication)].

¹²B. Muhlschlegel, D. J. Scalapino, and R. Denton, Phys. Rev. B **6**, 1767 (1972).

¹³M. C. Wang and G. E. Uhlenbeck, Rev. Mod. Phys. **17**, 323 (1945).

¹⁴Due to the equivalence of each particle in the necklace, all the diagonal elements $G_{ii}^N(\omega)$ are equal.

¹⁵In fact the fit to a single Lorentzian at $T \sim T_c$ is not as good as at other temperatures. In this region the effective Γ departs from the lowest normal-mode frequency Γ_1 and reaches the middle of the normal-mode band. The temperature interval for which this effect occurs is much narrower for the large-particle case which simulates a sharper bulklike transition (see Figs. 2 and 3).

¹⁶K. Maki, *Prog. Theor. Phys.* **31**, 731 (1964).

¹⁷The same parameter α_H defined by Eq. (4.1) was used in Refs. 4 and 7.

¹⁸We did not consider in our calculation the quantum effects due to the smallness of the particle; therefore, the present model does not apply to particles with $\delta > 1$.

In addition, when $\delta \sim 1$ the pair-breaking effect due to the diffusive (surface) scatterings becomes stronger than that of the field H . Hence, the expression (4.2) for α_H should contain an additional term $\alpha_0 \approx T_c/k_F R$, where R is the radius of the particle. (See, e.g., Ref. 2).

¹⁹The expression (4.3) was derived by Sone with a slight modification in the second term [see Eq. (55) of Ref. 7]. It is our belief that the pair-breaking effect was not treated self-consistently in this work. Our Eq. (4.3) simply neglects this effect.

²⁰Numerical calculations show that there is still a visible effect on $T_1(T)$ for $\alpha \approx 10^{-2}$.

²¹This effect could be treated as for the quasi-one-dimensional superconductors [e.g., see S. Cremer and E. Šimánek, *Phys. Rev. Lett.* **36**, 1272 (1976)].